An Amino-Substituted Phenylethynyl-anthracene Probe Shows a Sensitivity to Changes in the Lipid Monolayer Curvature of Nonlamellar Lipid/Water Phases

ARTICLE *in* THE JOURNAL OF PHYSICAL CHEMISTRY B · SEPTEMBER 2000

Impact Factor: 3.3 · DOI: 10.1021/jp993779b

3 AUTHORS, INCLUDING:

Borislav Angelov
Academy of Sciences of the Czech Republic
51 PUBLICATIONS **942** CITATIONS
SEE PROFILE

Angelina Angelova
Université Paris-Sud 11
88 PUBLICATIONS **1,678** CITATIONS
SEE PROFILE

An Amino-Substituted Phenylethynyl-anthracene Probe Shows a Sensitivity to Changes in the Lipid Monolayer Curvature of Nonlamellar Lipid/Water Phases

Borislav Angelov,[†] Angelina Angelova,*[,‡] and Radoslav Ionov[‡,§]

Institute of Biophysics, Bulgarian Academy of Sciences, Acad. G. Bonchev Str., Bl. 21, BG-1113 Sofia, and College of Sciences "Leonardo da Vinci", P.O. Box 946, BG-1000 Sofia, Bulgaria, and Institute of Applied Physics, Technical University, BG-1156 Sofia, Bulgaria

Received: October 25, 1999; In Final Form: May 12, 2000

The fluorescent excitation and emission spectra of an amphiphilic 2-amino-substituted bis(phenylethynyl)-anthracene derivative (APA) are studied in self-organized supramolecular assemblies of the hydrated lipids dipalmitoylphosphatidylcholine (DPPC), dioleoylphosphatidylethanolamine (DOPE), and monooleoylglycerol (MO), which form, under well-defined conditions, one-dimensional lamellar, two-dimensional inverted hexagonal, and three-dimensional inverted cubic structures, respectively. A comparison is made with APA spectra in organic solvents. Because the investigated fluorescent molecule is water-insoluble and is favorably located in the hydrocarbon-chain region proximate to the lipid headgroup/water interfaces of the host lipid/water structures, its spectral properties are anticipated to be influenced by the lipid monolayer curvature changes of the periodic nonlamellar organizations (as induced for instance by temperature changes). The results indicate that the temperature-induced variations of the excitation and emission maxima of APA in lipid phases are distinct from those in organic solvent and that the hydrophobic fluorophore is sensitive to the polarity of the microenvironment in the proximate vicinity of the headgroup region of the lipid assemblies. Correlations are established between the temperature dependences of the fluorescence maxima of APA and the temperature-induced changes in the curvatures of the lipid headgroup regions of the nonlamellar MO and DOPE lyotropic phases.

Introduction

Incorporation of chromophore species in organized microheterogeneous media of supramolecular periodicities[1−14] is of interest for the creation of novel sensor, energy storage, and molecular electronics devices[15,16] of small dimensions.[1−16] Advantages of lyotropic lipid/water phases, as microheterogeneous media for control of photophysical processes, chemical reactions, and tailoring of charge-transfer complexes or π-electron arrays,[15,16] are their well-defined composition, flexibility, anisotropic nature, and possibility for polarity modulation. Lipid-based supramolecular assemblies[17] may be organizaed as multilamellar[18] or tubular microstructures[19] as well as in nonlamellar inverted hexagonal or cubic packings.[17,20,21] As host structures,[18,22−24] lipid/water phases possess a high capacity to encapsulate various lipoidal (oil-soluble) or water-soluble species,[18,25,26] among which fluorescent and chemiluminescent dyes[8a,11c,12c,15,27−30] have been studied.

In the present study, the spectroscopic properties of an amphiphilic 2-amino-substituted bis(phenylethynyl)anthracene derivative (APA) embedded in hydrated lipid phases of diverse supramolecular organizations are investigated. The chemical structure of APA is shown in Figure 1. This dye is of a fundamental interest because it contains a polar amino group attached to a large, hydrophobic π-electron conjugated chromophore system.[31] The presence of a 2-amino group is essential for the environmental effects on the spectra. In addition, the hydrophobic−hydrophilic balance resulting from the chemical structure of APA indicates amphiphilic properties of the dye and solubility in lipid environment. Although APA is a water-insoluble derivative capable of forming monolayers upon spreading at the air/water interface,[24] it is of a crystalline character in a bulk state and exhibits a high thermal stability. Up to now, APA has only been incorporated in organized thin films[24]

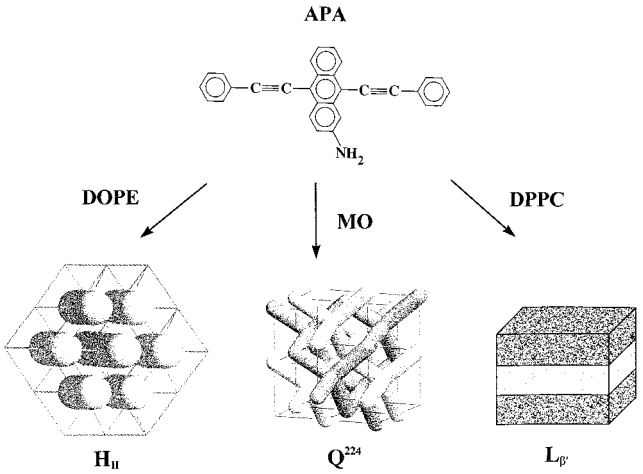

Figure 1. Top: Chemical structure of the amphiphilic fluorescence probe 2-amino-9,10-bis(phenylethynyl)anthracene (APA). Bottom: Schematic presentations of the supramolecular organizations of the lyotropic phases into which APA is incorporated. The investigated lipids DOPE, MO, and DPPC form an inverted hexagonal (H_{II}) phase, a bicontinuous inverted-cubic (Q^{224}) phase, and a lamellar bilayer gel ($L_{\beta'}$) phase, respectively, when hydrated in excess water. The indicated supramolecular organizations correspond to a temperature 20 °C.

* To whom correspondence should be addressed: E-mail: a-angelova@usa.net.

[†] Institute of Biophysics, Bulgarian Academy of Sciences.

[‡] College of Sciences "Leonardo da Vinci".

[§] Institute of Applied Physics, Technical University.

10.1021/jp993779b CCC: $19.00
Published on Web 09/09/2000

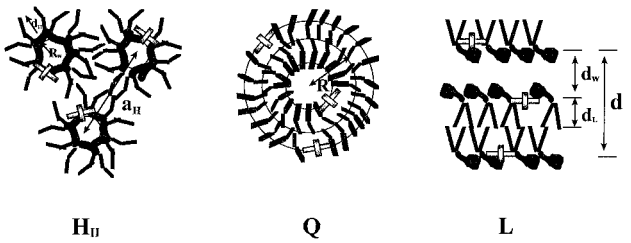

Figure 2. Cross-sectional views of the inverted hexagonal H_{II}, bicontinuous cubic Q and lamellar L structural elements and a suggested location of the cruciform-shaped fluorescent APA molecules in the curved or planar lipid monolayers of the nonlamellar (H_{II} and Q) or lamellar (L) supramolecular lipid/water structures. Notations: a_H = lattice parameter of the H_{II} phase, R_w = radius of the water tubes in the H_{II} phase, d_H = thickness of the lipid monolayers in the H_{II} phase, R = radius of the rodlike structural elements of the bicontinuous cubic phase, d = repeat spacing of the lamellar lipid/water phase, d_w = thickness of the aqueous layers in the lamellar lattice, and d_L = thickness of the lipid bilayers organized in a lamellar phase. In relative magnitudes, the radius of lipid monolayer curvature is small in the H_{II} phase, intermediate in the bicontinuos cubic (Q) phase, and infinitely large in the lamellar (L) phase. Generally, the changes in the lipid monolayer curvature with temperature result from the temperature-induced variations of the water-core radii of the tubes constituting the nonlamellar cubic and H_{II} phases.

but not in hydrated lipid structures. There is strong evidence that the supramolecular organizations of host lipid phases may essentially influence the properties of incorporated dye components.[10e,24,30]

The aim of this investigation is to determine the optical sensitivity of the novel 2-amino-substituted fluorescence probe APA to the physicochemical and structural features of selected lipid/water phases characterized by lamellar bilayer, inverted hexagonal, and bicontinuous cubic lattice periodicities. (The supramolecular organizations of the latter are schematically presented in Figure 1.) Organized amphiphilic media were created here by hydrating the lipids dioleoylphosphatidylethanolamine (DOPE), monooleoylglycerol (MO), and dipalmitoylphosphatidylcholine (DPPC) under excess water conditions. Lipid phases of known structures and mesomorphic phase behavior (see the Appendix) were prepared because it was a priori unknown by which means (polarity, lipid monolayer curvature, phase state) they will influence the new 2-amino-substituted chromophore studied. Excitation and emission spectra of APA were investigated as a function of temperature either in organic solvents or in the organized supramolecular environments of DOPE, MO, and DPPC. The sensitivity of the spectral characteristics of the dye to the host microenvironments and the properties of the lipid superstructures are demonstrated.

Location of the Fluorescent Dye APA in Hydrated Lipid Assemblies of Lamellar and Nonlamellar Supramolecular Organizations. The location of the APA molecules in the supramolecular organizations of fully hydrated lipid (DOPE, MO, or DPPC) phases could be considered as nearly fixed at their polar/apolar interfaces (Figure 2). This location was suggested considering that APA (i) is a substance that is insoluble in the aqueous phase and is of an amphiphilic nature;[24] (ii) contains a large hydrophobic chromophore, comprising an anthracene core and two phenylethynyl substituents, which prefers a hydrophobic environment and a location in the acyl-chain regions of the lipid assemblies; (iii) possesses a polar, ionizable[34] amino group, which requires a polar environment in the lipid dispersions and a contact with the aqueous phase; (iv) has the appropriate stereochemical structure and molecular size. (The dimensions of the platelike APA molecule (Figure 1), determined from its molecular model, are 16.6 Å in width (*x*-axis) and 9.5 Å in height (*y*-axis); the thickness of the molecule in the side orientation is 3.5 Å (*z*-axis)). In Figure 2, the fluorophore moiety of APA is considered to be fixed within the hydrophobic hydrocarbon-chain portion proximate to the polar/apolar interfaces of the lipid assemblies. In fact, most of aromatic dyes locate preferably at the polar/apolar interfaces of amphiphilic supramolecular structures.[35]

Lamellar phases (L), like those characteristic of the investigated DPPC, are of zero curvature of their structural elements (Figure 2). The curved structural elements of the nonlamellar phases of fully hydrated DOPE (H_{II} phase) and MO (Q phase) (Figure 2) display a monolayer curvature that is temperature dependent (see Figure 9 in the Appendix). It may be assumed that at the low dye/lipid molar ratio (1:250) studied, the APA molecules incorporated in host lipid phases do not alter their phase states and do not destabilize their supramolecular organizations. Our recent study of two-component APA/lipid monolayers[24] has demonstrated that mixing of APA with lipid species at fluid interfaces does not cause essential perturbation of the lipid molecular packing at low dye/lipid molar ratios.

Materials and Methods

Chemicals. The phospholipids 1,2-dipalmitoyl-*sn*-glycero-3-phosphatidylcholine (DPPC) and 1,2-dioleoyl-*sn*-glycero-3-phosphatidylethanolamine (DOPE) were from Avanti Polar Lipids Co., and their purity was higher than 99%. 1-Monooleoylglycerol (MO, monoolein) and the fluorescence probe 2-amino-9,10-bis(phenylethynyl)anthracene (APA) (99%, mp252 °C) were purchased from Sigma-Aldrich Co. Anhydrous organic solvents *N*,*N*-dimethylformamide, tetrahydrofuran, diethyl ether (diethylene oxyde), and chloroform or methanol of a UV−Vis spectroscopic grade (Fluka) were used (APA was poorly soluble in hexane and cyclohexane). An aqueous phosphate buffer solution with a concentration 10^{-2} M and pH 7.0 was prepared using the inorganic salts NaH_2PO_4 and Na_2HPO_4 (p.a. grade, Merck) and doubly distilled pure water. All of the preparations described below were performed under dark conditions.

Preparation of Hydrated Lipid Phases with Incorporated Dye Molecules. Homogeneous dye/lipid mixtures of a molar ratio 1:250 were obtained as follows: Lipids (dry powders) were dissolved in chloroform to a concentration of 3 mg/mL. APA (crystalline powder) was dissolved in the same organic solvent to the concentration necessary to achieve the desired dye/lipid molar ratio. Chloroform was then evaporated under stream of nitrogen gas for about 30 min, followed by exposing the samples under low vacuum (10^{-2} Torr). This helped the residual organic solvent to be entirely eliminated, after about 14 h at room temperature. To prepare lyotropic (lipid/water) phases with an incorporated component APA, dry dye/lipid mixtures were hydrated in excess aqueous buffer phase to a total lipid concentration of ~ 0.4 wt % in water. The hydration was done at a temperature 50 °C by incubation of the samples in water bath for 20 min. Subsequent eight cycles, consisting of vigorous vortexing for 1 min, 15 s sonication in water-bath sonicator (at a frequency of 50 Hz), and incubation for 4 min at 50 °C, were performed for both DOPE and MO. For the hydration and homogeneous dispersing of the APA/DPPC mixture in aqueous solution, there was no need of a sample sonication. The applied procedure allowed preparation of lipid/dye supramolecular structures finely dispersed in water. The samples were equilibrated for 1 h and filled in spectroscopic quartz cuvettes with 2 mm thickness.

Spectroscopic Experiments. Fluorescence excitation and emission spectra of APA either in organic solvent or in

organized lipid media were measured by means of an equipment consisting of a SPEX monochromator and a cooled photomultiplier. Steady-state excitation and emission measurements with a reference hydrated-lipid sample, which did not contain APA molecules, gave negligibly small optical signals. The wavelength resolution was 1 nm. For excitation spectrum measurements, the APA probe incorporated in lipid phases was excited with light in the spectral range from 300 to 580 nm and the emission was measured at a wavelength of 590 nm. The APA probe in organic solution had an excitation range from 300 to 520 nm and emission at 530 nm or higher. For emission spectrum measurements, the APA/lipid samples were excited with light at 530 nm, and the emission spectra were recorded from 550 to 620 nm. For APA dissolved in solvent, the excitation wavelength was 480 nm, and the emission range was from 490 to 700 nm, respectively. The data were collected with cuvettes positioned at an angle of 45° with respect to the incident excitation beam in order to avoid scattering of light. The fluorescent instrument was not corrected for wavelength dependence of the excitation intensity. Taking into account the wavelength range in which APA fluoresces, the latter does not have a dramatic influence on the emission spectra. The positions of the peaks maxima, λ_{max}, were determined from the condition of zero first derivatives of the spectral profiles. A procedure of peaks smoothing (Savitzky-Golay method) was applied when necessary.

The fluorescent properties of the APA probe were monitored as a function of temperature both in organic solvent and in lipid environments. The temperature of the sample compartment was varied within the range from 0 to 55 °C. The thermostated cuvette holder was connected to a thermocouple and an external thermostat. The fluorescence spectra were recorded stepwise with temperature steps of 5 °C. The samples were allowed to equilibrate for about 10 min at every temperature step in the investigated range from 0 to 55 °C. To keep the samples homogeneity, the lipid dispersions were vortexed shortly prior to the fluorescent measurements.

UV−Vis absorption spectra of APA in spectroscopic-grade organic solvents were measured by means of a Perkin-Elmer Lambda 9 UV−Vis spectrophotometer with a wavelength resolution of 2 nm. Quartz cuvettes of 10 mm thickness were used. At the employed APA solution concentration, around 5×10^{-6} M, dye self-aggregation in the organic solvent medium was not detected. Self-quenching of the dye emission and spectral shifts due to self-aggregation of the dye in solution were observed at APA concentration 10^{-3} M.

Results and Discussion

UV−Vis absorption spectra. UV−Vis absorption spectra of 2-amino-9,10-bis(phenylethynyl)anthracene (APA) were measured in the organic solvents diethyl ether (Et_2O), dimethylformamide (DMF), tetrahydrofuran (THF), chloroform (CH_3Cl), and methanol (MeOH). The wavelengths of the main absorption maxima (λ_{max}) obtained at 20° C are given in Table 1. For instance, APA monomers dissolved in THF are characterized by spectral maxima around 284, 314, 397, and 485 nm. Figure 3 shows the absorption spectra of APA in Et_2O (1), THF (2), and DMF (3) solutions.

The performed solvent study indicates an essential dependence of the first singlet (S_o-S_1) electronic transition of APA on the environmental polarity. Although the maximum of the corresponding spectral band (which is of a longest wavelength) in the range between 476 and 503 nm is largely sensitive to the solvent polarity, the rest of the absorption bands (in the range 280−410 nm) are considerably less solvent dependent because they are of a different nature.

TABLE 1: Wavelengths λ_{Max} of Maximum UV−Vis Absorption and Fluorescence Emission (Flu) of 2-amino-9,10-bis(phenylethynyl)Anthracene (APA) in Organic Solvents[a]

solvent	ϵ[b]	type of solvent	λ_{max} (UV−Vis) (nm)				λ_{max} (Flu)[c] (nm)
Et_2O	4.335	dipolar	282	313	394	481	559
THF	7.6	dipolar	284	314	397	485	573
DMF	36.7	proton acceptor	288	317	401	503	597
MeOH	32.63	proton donor and acceptor	281	312	395	479	n.m.
CH_3Cl	4.806	nonprotic	283	315	394	476	537

[a] The λ_{max} values were determined from spectra measured at a temperature 20 °C and APA solution concentration around 5×10^{-6} M. Notations: ϵ = dielectric constant, Et_2O = diethyl ether, THF = tetrahydrofuran, DMF = dimethylformamide, CH_3Cl = chloroform, MeOH = methanol, n.m. = not measured. [b] Values[36] at 20 °C. [c] Determined at an excitation wavelength 480 nm.

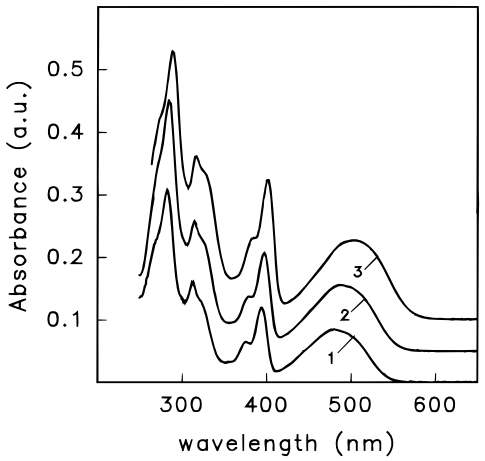

Figure 3. UV−Visible absorption spectra of the probe APA (~5×10^{-6} M solutions) in diethyl ether (1), tetrahydrofuran (2), and *N*,*N*-dimethylformamide (3). The spectra are shifted on the *Y*-axis for clarity.

The solvent dependence of the absorption maxima of a model compound with the same electron cloud as APA but lacking the 2-amino group (i.e., the unsubstituted bis(phenylethynyl)-anthracene) has been previously studied.[32a] The absorption spectra in the absence of 2-amino group show λ_{max} equal to 440 nm (in chloroform) and 438 nm (in dioxane). The comparison of these values with those in Table 1 suggests that the attachment of the electron-donating 2-aminogroup to the bis-(phenylethynyl) chromophore is essential for the shifts of the absorption maxima and the environmental effects on the spectra.

Fluorescence Spectra. The fluorescence excitation and emission spectroscopic properties of the 2-amino substituted APA derivative were studied in either organic solutions or in lipid assemblies of diverse lyotropic phase states and physicochemical properties. Strong fluorescence, originating from the large, delocalized π-electron system of the chromophore moiety, was established. It determines a high quantum yield of fluorescence equal to 0.58 in chloroform solution.[24] Exemplary plots of the fluorescence excitation (1) and emission (2) profiles of APA are presented in Figure 4. Such experimental data were collected (in host lipid phases or in solutions) at various constant temperatures between 0 and 55 (in steps of 5 C).

The L_a bands of the aromatic anthracene core are in the range 330−430 nm and are weakly solvent dependent. The L_b band is around 280 nm (not shown in Figure 4) and is also invariant of solvent. The band with a maximum around 500 nm is identified as the charge-transfer (CT) band and involves charge transfer from the aminogroup to the aromatic system, important

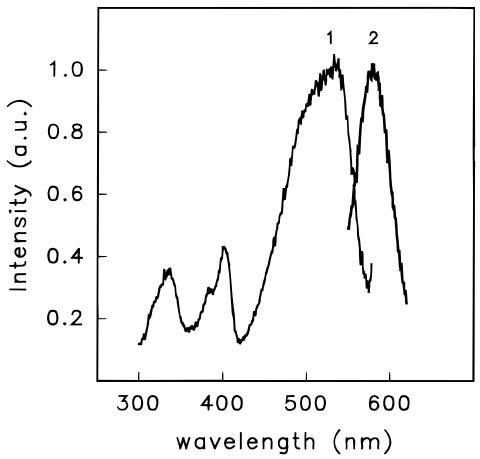

Figure 4. Normalized excitation (1) and fluorescence emission (2) spectral profiles of APA incorporated in a hydrated DOPE sample. The temperature is 15 °C.

solvent reorganization and perhaps a rehybridization of the nitrogen. Hence, it is expected that this band is strongly dependent on the solvent type and lacks a fine structure. Solvent dependence is indeed established for the main excitation (CT) band as well for the fluorescent band (see the values of the wavelengths of maximum fluorescence λ_{max} in Table 1).

To demonstrate the effect of the 2-amino group on the fluorescence properties of the chromophore, the results obtained for APA were compared with the fluorescence λ_{max} values determined with the unsubstituted bis(phenylethynyl)anthracene compound (not possessing an amino group).[32a] The excitation maxima of the latter are around 467 nm (in chloroform) and 465 nm (in dioxane). The fluorescence emission has maxima at 475 nm (in chloroform) and 474 nm (in dioxane).

The temperature effect on the λ_{max} of APA fluorescence in organic solutions was marginal in the interval from 0 to 55 °C. For the APA fluorescence in DMF solution, λ_{max} decreased from 598 nm (at 5 °C) to 596 nm (at 55 °C), i.e., the shift $\Delta\lambda_{max}$ was only 2 nm. For APA fluorescence excitation in chloroform, the spectral shifts $\Delta\lambda_{max}$ was 3 nm (toward lower wavelengths) over the temperature interval of 50 °C (see Figure 5d).

Figure 5 shows the temperature dependences of the excitation spectra of APA in diverse host phases. Analogous plots were generated for the temperature dependences of the fluorescence emission bands (results not shown here). It was found that the spectra of APA monomers embedded in lipid phases are distinct from those in the organic solvent media. The slopes of the obtained λ_{max} versus temperature dependences (if approximated as linear plots) in lipid/water phases (see below) were essentially different in magnitude from those in organic solvents, thus suggesting that the observed effects are not due to trivial changes in the dielectric constant with solvent.

The performed investigation reveals that the spectroscopic characteristics of APA incorporated in lipid/water phases are sensitive to at least two effects of (i) the polarity of the lipid headgroup region at a constant temperature and of (ii) the temperature.

1. **Effect of the Lipid Headgroup Polarity at a Constant Temperature.** The positions of the excitation CT band of APA in hydrated MO, DOPE, and DPPC phases are compared at a constant temperature 20 °C in Figure 6a. The values of λ_{max} of excitation are red shifted in the sequence APA/MO (500 nm) < APA/DOPE (531 nm) < APA/DPPC (542 nm). The same trend of λ_{max} increase was observed at every temperature studied between 0 and 55 °C.

The fact that APA is influenced by the type of the lipid headgroups, and hence is in a contact with the hydrated polar headgroup regions of the investigated lipid/water phases, is demonstrated also by the observed red solvatochromic shift of its fluorescence emission band (Figure 6b). Figure 6b shows that the shift of the position of the emission maximum toward longer wavelengths follows the order APA/MO (λ_{max} = 573 nm) < APA/DOPE (λ_{max} = 578 nm) < APA/DPPC (λ_{max} = 582 nm).

As reviewed,[29c,30b] the wavelength of maximum emission, λ_{max}, shifts toward shorter wavelengths when a probe goes to a less polar or a less hydrated environment. Taking into account this phenomenological relationship, the observed red shifts of λ_{max} of the excitation and fluorescence bands of APA at a constant temperature (Figure 6) suggest that APA experiences a more polar environment in the sequence: MO < DOPE < DPPC.

Data on surface dielectric constants (ϵ_s) of hydrated lipid structures and membranes have scarcely been reported.[37] Generally, the ϵ_s characteristics of lipid bilayers fall in the range[37a−c] between 4 and 35 which is intermediate in a value between that[34d] of the hydrophobic hydrocarbon-tails interior ($\epsilon\sim2$) and that of the aqueous surrounding ($\epsilon\sim81$). If the APA chromophore was entirely embedded in the hydrophobic interior of the lipid assemblies, then it would have experienced a hydrophobic surrounding of a same low polarity ($\epsilon\sim2$) that would lead to the observation of same λ_{max} values in every lipid supramolecular structure studied. However, the λ_{max} values of excitation and fluorescence bands of APA do shift upon changing the polarity and hydration of the lipid headgroup regions (it is known that the DPPC, MO, and DOPE phases contain different amounts of water and are characterized by different degrees of hydration of the lipid headgroups[37d]). Since APA is sensitive to the properties of the polar/apolar interfaces of the host lipid/water phases, it appears to be indeed located in their interfacial regions as suggested in Figure 2.

It may be supposed that the surface dielectric constants,[34d,37] ϵ_s, of the headgroup/water interfaces of the investigated lipid phases follow the sequence: ϵ_s (MO) < ϵ_s (DOPE) < ϵ_s (DPPC). In addition, it could be noted that the excitation λ_{max} value of APA embedded in a MO/water phase (500 nm) is close to that (503 nm) of APA in a DMF solution (the DMF environment is characterized by ϵ = 36.7). The established sensitivity of the APA spectra to the lipid headgroups' polarity confirms that the dye molecules are not segregated into a separate domain but appear to be dispersed within the lipid phases.

2. **Effect of Temperature.** A detailed analysis was performed of the thermal behavior of the four bands, observed around 332, 384, 401, and 532 nm, in the excitation spectra of APA embedded in lyotropic phases of DOPE (a), DPPC (b), and MO (c) (Figure 5). The first band, positioned at ~332 nm in lipid/water phases, was almost invariant of temperature. The temperature dependence of the second excitation band (λ_{max} around 384 nm) was also marginal for all lipid types. The third excitation band showed a systematic decrease of λ_{max} with the rise of temperature for all lipid phases. For the hydrated DOPE and DPPC phases, the absolute decrease of λ_{max} with rising the temperature, $\Delta\lambda_{max}$, was 4 nm in the interval from 0 to 55 °C, whereas for APA excitation in the MO/water phase $\Delta\lambda_{max}$ was 2 nm. Most significant temperature influence was found on the λ_{max} values of the fourth (CT) excitation band as well as on the emission band.

Figure 7 presents the temperature-induced variations of the wavelengths λ_{max} of the main excitation (a) and the fluorescence

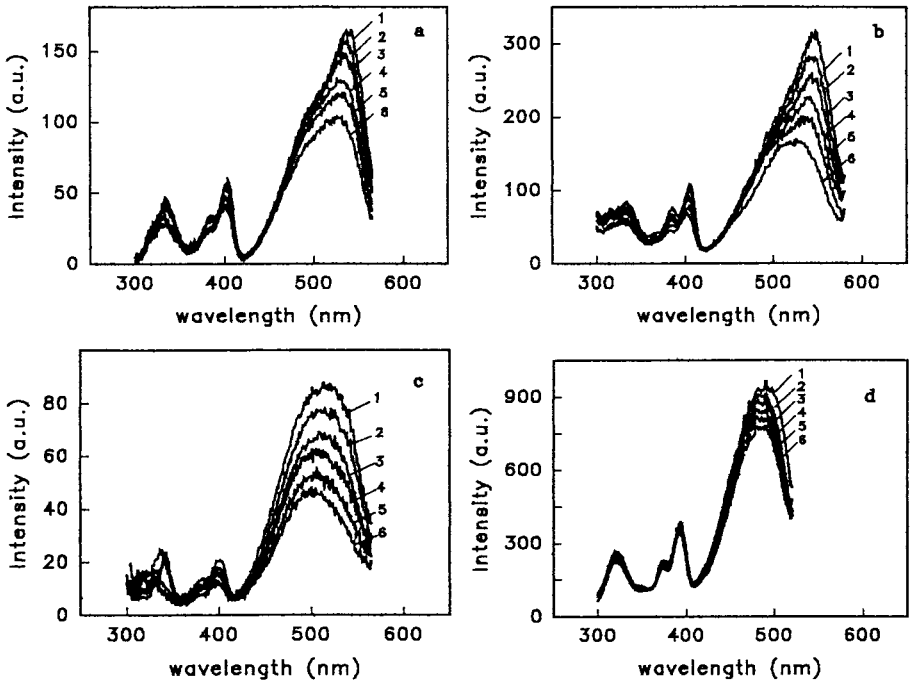

Figure 5. Temperature dependences of the excitation spectra of APA studied in the interval from 0 and 55 °C. APA is incorporated in DOPE (a), DPPC (b), and MO (c) aqueous dispersions or dissolved in organic solvent (5×10^{-6} M chloroform solution) (d). The presented spectral profiles correspond to temperatures of 0 °C (1), 10 °C (2), 20 °C (3), 30 °C (4), 40 °C (5), and 50 °C (6). The increase of temperature caused a shift of the main excitation maximum to shorted wavelengths.

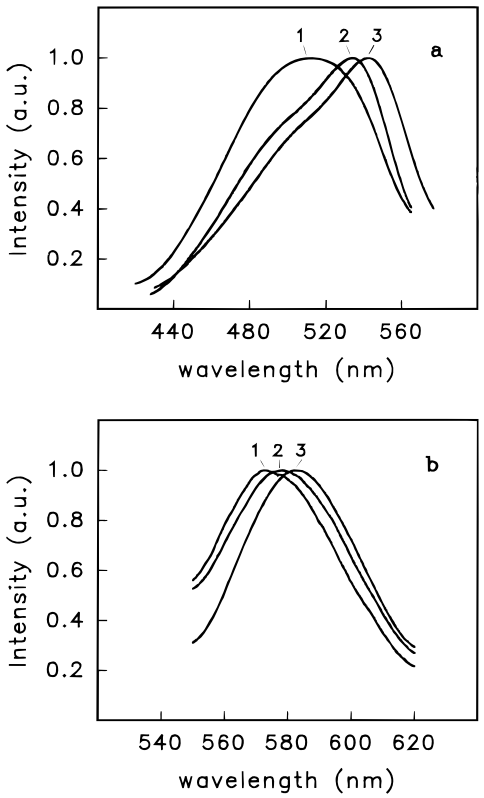

Figure 6. Comparison of the positions of the main excitation (a) and fluorescence emission (b) maxima of APA in normalized spectra recorded at a constant temperature (20 °C) in supramolecular structures of fully hydrated MO (1), DOPE (2), and DPPC (3). The excitation of APA incorporated in lipid/water phases was at 530 nm.

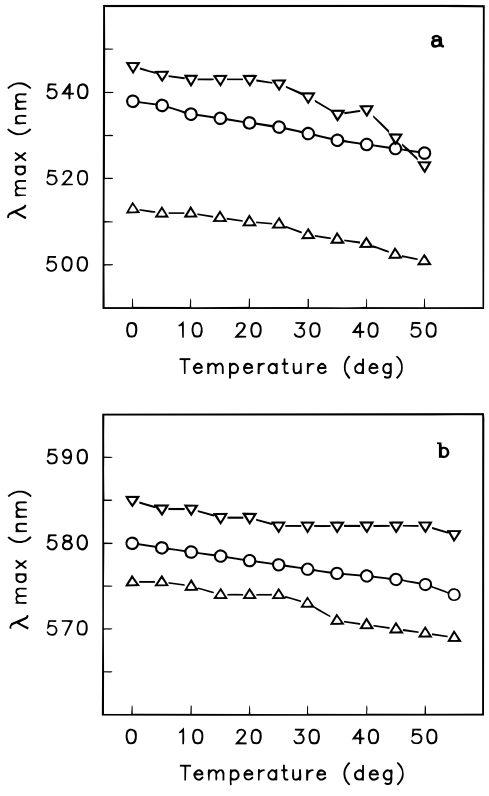

Figure 7. Wavelength (λ_{max}) of maximum excitation (a) or emission (b) vs temperature plots determined for APA fluorescence in organized media of fully hydrated MO (△), DOPE (○), and DPPC (▽).

emission (b) bands of APA in the different lipid media studied. The obtained dependences are of negative slopes, i.e., the λ_{max} values shift toward shorter wavelengths upon rising the temperature.

The dependences of the APA excitation and emission maxima on temperature could be due to the temperature-induced changes in the structural features of the periodic lipid assemblies, which alter the hydrophobicity of the local surrounding of APA.

2.1. *APA in DOPE Dispersions.* A correlation is found between the temperature-induced change in the optical charac-

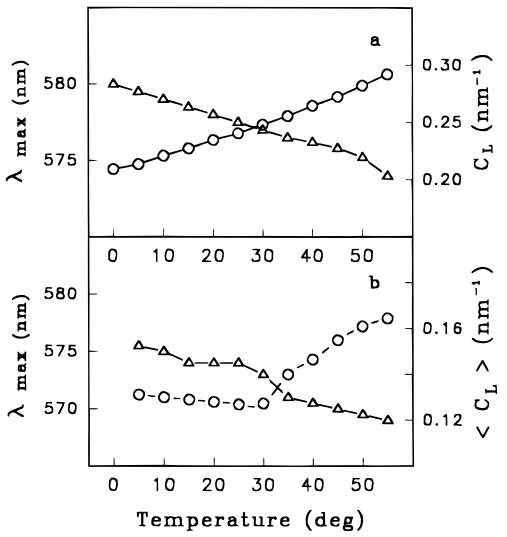

Figure 8. Correlations of the temperature-induced changes in the wavelength λ_{max} of fluorescent emission of APA (triangles) in nonlamellar lipid phases and the mean curvature of the lipid headgroup/water interfaces, C_L (circles), in H_{II}-phase DOPE (a) and in Q^{224} cubic phase MO (b) structures.

teristics of APA chromophore embedded in an H_{II}-phase DOPE structure (Figure 7) and the continuous increase in the mean curvature of the structural elements of the host supramolecular organization (see the Appendix for the estimation of the mean monolayer curvature, C_L, in an H_{II}-phase). The correlation is demonstrated in Figure 8a for the case of APA fluorescence in a DOPE dispersion. The monotonic increase in C_L with temperature is associated with a progressive blue shift of the emission maximum of the embedded fluorescent probe. A similar correlation is valid also for the excitation maxima of APA incorporated in a H_{II}-phase DOPE matrix.

It has been suggested[17,30d] that upon transition of lipids into a H_{II} phase, the water content of the lipid structure is reduced and that the $L_\alpha - H_{II}$ phase transition is accompanied by dehydration of the lipid headgroup surfaces. As a result of the thermally induced change in the lipid monolayer curvature of the H_{II} phase, the hydrophobic/hydrophilic balance of the polar headgroups/water interfaces alters with the temperature increase. The polarity of the environment of the incorporated fluorescent probe is thus modified owing to the variation of the depth of penetration of water molecules into the lipid headgroup region and the continuous dehydration of the headgroups upon heating. Therefore, the increase of temperature should lead to blue shifts of the excitation and fluorescence maxima of APA as it is experimentally observed with the APA/DOPE systems (Figure 7, circles).

2.2. *APA in MO Dispersions.* Figure 8b presents the correlation between the fluorescence λ_{max} versus temperature dependence and the mean monolayer curvature, $\langle C_L \rangle$, versus temperature plot obtained for APA incorporated in an MO bicontinuous cubic organization (for the calculation of $\langle C_L \rangle$ see the Appendix). The fluorescence λ_{max} versus temperature plot changes its slope at about 30 °C, where changes in the mean curvature of the lipid headgroup regions are induced upon heating.

The λ_{max} versus temperature profiles for both APA excitation (Figure 7a, triangles) and emission (Figure 7b, triangles) are of negative slopes in the nonlamellar MO/water system. The established blue shifts during heating suggest that the polarity of the environment of the APA chromophore decreases upon rising the temperature. This result indicates that the molecular probe is exposed to a less polar environment at temperatures above 30 °C, which might be caused by the progressive dehydration of the lipid headgroup surfaces. In fact, changes in the lipid monolayer curvature with temperature lead to associated changes in the number of water molecules at the places of location of the APA chromophores. In addition, the increase in the hydrophobicity of the APA surrounding in the investigated nonlamellar structures could be caused by rearrangement of the lipid molecules, which is thermally stimulated by heating.

2.3. *APA in DPPC Dispersions.* The spectroscopic results demonstrate that the slope $d\lambda_{max}/dT$ for the fluorescence of APA in the lamellar-phase DPPC dispersion is almost negligible in value (Figure 7b, inverted triangles). The APA molecules are rigid in nature, and the modification of their fluorescence response (related to dipole−dipole interactions with the environment in the excited state of the chromophore) appears to be very small upon the temperature-induced gel-to-fluid phase transition of DPPC. At variance, the λ_{max} versus temperature dependence for the excitation of APA in lamellar DPPC phases (Figure 7a, inverted triangles) changes its slope at the temperatures that approximate the crystalline-to-gel and the gel-to-fluid phase transition temperatures of the hydrated lipid system. These λ_{max} alterations and the associated dipole−dipole interactions in the ground state of the chromophore could reflect the lipid molecular rearrangement during the crystalline-to-gel and gel-to-fluid structural phase transitions of DPPC.

The temperature-induced changes in the structural parameters (d and d_w) of the lamellar phases of hydrated DPPC (see Figure 2 and the Appendix) do not lead to as significant effects on the fluorescence characteristics of the embedded APA molecules as it is established with the nonlamellar DOPE and MO structures. As previously reviewed,[30d] lamellar−lamellar phase transitions, as those characteristic of DPPC dispersions, do not cause essential alteration of the hydration of the lipid headgroups. Hence, the degree of water penetration into the local surrounding of APA in the lamellar-phase DPPC structures is not expected to significantly vary upon rising the temperature. As a result of unchanged hydration of the polar headgroup region upon heating, λ_{max} of fluorescence emission of APA appears to be weakly temperature dependent in the lamellar DPPC organizations.

Therefore, the established temperature effect on the APA spectral maxima in nonlamellar lipid environment could be realized, suggesting that APA is a fluorescent probe sensitive to changes in the lipid monolayer curvature and to the associated alterations of the interfacial polarity and hydration of the lipid headgroup region.

Comparison with Other Fluorescent Dyes Probing the Properties of Nonlamellar Lipid Phases. The incorporation of dyes in nonlamellar lipid phases has been recently reported.[28,30] Fluorescent probes, which are sensitive to the solvent polarity, have been suitable for studies of bilayer-to-hexagonal phase transitions of lipids.[28,30] For instance, lipophilic dimethylaminocoumarin dyes (TMAC and DTMAC) as well as water-soluble probes (N^ϵ-dansyl-L-Lys (DNS-Lys) and the aminonaphthalene probe Laurdan) have been used in the investigation of the $L_\alpha - H_{II}$ transition of dipalmitoleoyl phosphatidylethanolamine (DiPOPE).[30a] The conclusion about the change in the surface polarity of the lipid headgroups upon approaching the bilayer-to-hexagonal transition temperature of the lipid has been dependent on the proximity of the employed chromophores to the curved DiPOPE headgroup/water interfaces.

An essential difference in the chemical structures of the above dyes[28,30] and the investigated APA probe is that the chromophore of APA comprises the hydrophobic, rather than the hydrophilic,

portion of the molecule. Because of the particular and well-defined interfacial location of this relatively large chromophore moiety, the spectral maxima of APA show a pronounced sensitivity to the changes in the curvatures of the lipid headgroup regions of the nonlamellar DOPE/water and MO/water phases.

To our knowledge, this is the first study in which correlations were deduced (Figure 8) between the temperature dependences of the wavelengths of maximum fluorescence of a molecular probe incorporated in supramolecular lipid organizations and the mean curvatures of the headgroup/water interfaces of nonlamellar lipid phases. The established spectral shifts $\Delta\lambda_{max}$ of APA fluorescence emission and excitation with rising the temperature in nonlamellar lipid structures are suggested to result from temperature-induced variations of the lipid monolayer curvature and the associated changes in the hydration and polarity of the lipid headgroup region.

Conclusion

The spectroscopic results suggest that the investigated 2-amino-substituted bis(phenylethynyl)anthracene derivative APA incorporates easily into organized lipid structures. The probe is characterized by intensive absorption and fluorescence bands. Due to its chemical structure and steric dimensions, the amphiphilic APA molecule is considered to be located at the apolar/polar interfaces of the host lipid/water phases and to be partially exposed to both the hydrophobic chain domain and the polar headgroup region of the host supramolecular lipid assemblies. Thus, APA appears to be sensitive to the local polarity of the environment in a portion of the lipid headroup region. Upon changing the host medium, red shifts were observed of the excitation and emission maxima of APA, which indicate that the environmental polarity increases in the order MO < DOPE < DPPC. Because APA shows a sensitivity to the dielectric constant of its environment, it may be regarded as an "environment-sensitive" probe.

In addition to environmental sensitivity, the main excitation and fluorescence emission bands of APA display temperature dependences that differ for the nonlamellar and the lamellar host lipid/water phases and are distinct from those in organic solutions. Correlations were found between the blue shifts of λ_{max} upon heating and the temperature-induced increase in the mean curvatures of the lipid monolayers in the inverted hexagonal (DOPE/water) and the bicontinuous cubic (MO/water) structures. This result suggests that APA could be regarded as a molecular probe that may detect changes in the curvature and the interfacial hydrophobicity of nonlamellar lipid structures induced for instance by temperature variations.

Appendix

Temperature Dependence of the Lipid Monolayer Curvatures of the Nonlamellar Lipid/Water Phases Estimated from Known Structural Data. The temperature effect on the polymorphic phase states and the structural lattice parameters of the lipid/water phases formed upon hydrating DOPE, MO, or DPPC in excess aqueous environment has been documented in literature.[21c,38−41] Fully hydrated DOPE exhibits a characteristic temperature-induced lamellar-to-nonlamellar phase transition[38,39] with a phase transition temperature from a lamellar (L_α) bilayer to an inverted-hexagonal (H_{II}) phase state, T_h, in the range between 3 and 13 °C. Under the conditions investigated here, T_h was 3 °C and above this temperature only the H_{II} phase was present in the DOPE dispersion.[39b] Upon hydrating in excess aqueous phase above 0 °C, mono-olein spontaneously self-assembles into a bicontinuous Q^{224} cubic phase[21c,40] (of the crystallographic space group *Pn*3*m*). Within the temperature interval from 5 to 92 °C, the MO cubic lattice parameter varies[40a] from about 10.5 nm (at 5 °C) to about 7.1 nm (at 92 °C). The lattice parameter, a_Q, is nearly constant within the temperature range from 5 to 30 °C followed by a continuous decrease at higher temperatures (see Figure 3 of ref 40a). Depending on temperature, DPPC forms diverse lamellar lyotropic phases in excess water,[41] such as a crystalline (L_c) phase, a gel ($L_{\beta'}$) phase, a ripple ($P_{\beta'}$) phase, and a liquid-crystalline (L_α) phase. The main transition from a gel state ($P_{\beta'}$) to a liquid-crystalline (L_α) phase occurs at about 41.5 °C. The temperature of the pretransition ($L_{\beta'}-P_{\beta'}$) of the hydrated phospholipid is around 35 °C and that of its subtransition ($L_c-L_{\beta'}$) is around 17 °C. The long-range ordering of DPPC aqueous dispersions is due to the stacking of lipid bilayers into lamellar structures. The bilayers are separated from each other by a layer of water (with a thickness d_w) (see Figure 2, right). The repeat unit, *d*, of the lamellar structures contains one lipid bilayer (with a thickness $2d_L$). Upon rising the temperature, the repeat spacing (*d*) of the lipid supramolecular organization of the hydrated DPPC takes characteristic values[41] of 5.97 nm (L_c phase at 15 °C), 6.4 nm ($L_{\beta'}$ phase at 20 °C), 7.2 nm ($P_{\beta'}$ phase at 40 °C), and 6.65 nm (L_α phase at 43 °C).

Inverted Hexagonal Phase (Fully Hydrated DOPE). In the H_{II} phase, the lipid (DOPE) molecules are organized as monolayers curved around nearly-cylindrical water tubes (see the structure drawn in Figure 1). The nearest-neighbor distance of the water-core centers of the cylindrical lipid aggregates arranged in a hexagonal packing is determined by the lattice parameter, a_H, of the H_{II} phase (see the definitions of the structural parameters in Figure 2). For the investigated temperature range and aqueous phase conditions (pH 7.0), it has been determined by X-ray diffraction[39b] that a_H of fully hydrated DOPE decreases continuously from 8.1 nm at 0 °C to about 6.8 nm at 55 °C. According to ref 38a, it is the radius of the water cylinders, R_w, of the H_{II} phase (see R_w in Figure 2), respectively, the radius of lipid monolayer curvature,[42] that mainly changes upon the increase of temperature. The thickness of the lipid monolayers forming the H_{II} phase, d_H, has been found to be weakly temperature dependent and to decrease by less than 0.1 nm over a temperature interval of 50 °C.

The mean curvature, C_L, of the lipid headgroup/water interfaces in the H_{II} phase of DOPE was determined using the relationship:[43a]

$$C_L = (2R_W)^{-1} \tag{1}$$

The calculation required the radius of the water tubes, R_w, in the H_{II} phase to be estimated at every temperature from the lattice parameter[39b] a_H of the H_{II} structure

$$R_w = a_H\sqrt{\sqrt{3}(1 - f_L)}/\sqrt{2\pi} \tag{2}$$

This computation assumes a circular shape of the cross section[43b,c] of the aqueous tubes (Figure 2)). In eq 2, f_L is the lipid volume fraction defined as[43b]

$$f_L = \left[1 + \frac{(1 - c_L)\upsilon_W}{c_L\upsilon_L}\right]^{-1} \tag{3}$$

where υ_w and υ_L denote partial specific volumes of water and lipid, and c_L represents the lipid weight fraction. The values of f_L were taken at limited hydration of the lipid.[38a] The density of DOPE, ρ_L, is 1.019 g/cm^3 at 20 °C, and its temperature

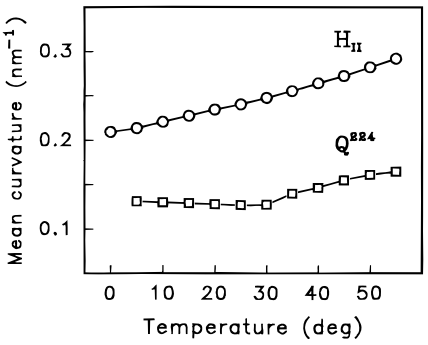

Figure 9. Temperature dependences of the mean curvatures of the headgroup/water regions of DOPE (circles) and MO (squares) monolayers calculated from the temperature dependences of the structural dimensions of the corresponding inverted hexagonal (H_{II}) and bicontinuous cubic (Q^{224}) phases of the hydrated lipids.

dependence was assumed to be $\rho_L(T) = \rho_{L20}\,[1-9\times10^{-4}\,(T-20)]$, where T is temperature. For H_{II}-phase DOPE, it was estimated that R_w changes continuously from about 2.39 nm to about 1.71 nm in the temperature interval from 0 to 55 °C.

Figure 9 (circles) shows the obtained temperature dependence of the mean curvature, C_L, of the lipid headgroup/water interfaces in the inverted-hexagonal phase structure of DOPE. The plot indicates that the decrease in R_w with the rise of temperature results in a progressive increase in the mean curvature at the DOPE monolayer headgroup/water interfaces in the H_{II}-phase arrangement.

Cubic Phase (Fully Hydrated MO). The structure of the Q^{224} cubic phase (schematically drawn in Figure 1) consists of two independent networks of aqueous tubes joined four-by-four at tetrahedral angles.[21c] Every tube in the continuous channel system is surrounded by a lipid bilayer, which separates the aqueous phase from the hydrocarbon continuum in the supramolecular lipid organization (Figure 2, middle).

For the investigated temperature range, the mean curvature, $\langle C_L\rangle$, at the lipid headgroup/water interface in the Q^{224} cubic phase of MO was calculated here from the cubic lattice parameter, a_Q, and the lipid length, l, according to the relationship:[43a]

$$\langle C_L\rangle = -2\pi\chi\, l/(\sigma\, a_Q{}^2 + 2\pi\chi\, l^2) \qquad (4)$$

The lipid length, l, and the dimensions of the structural elements of the MO bicontinuous cubic phase were determined on the basis of the structural formalism developed by Luzzati.[21c,d,43b,c] This formalism assumes that the Q^{224} cubic cell volume, $a_Q{}^3$, contains four rods of a circular cross section ($a_Q{}^3 = 4\,V_{rod}$). The volume occupied by each rod, V_{rod}, is derived as

$$V_{rod} = \pi\, R^2 l_{rod}\,(1 - k_V\, R/l_{rod}) \qquad (5)$$

where R is the rod radius and l_{rod} is the rod length ($l_{rod} = \lambda\cdot a_Q$). For Q^{224} phase, $k_v = 0.780$ and $\lambda = \sqrt{3}/2$ (see ref 43c). Then, the radius of the rods, R, was determined by solving the cubic equation

$$a_Q{}^3 = 2\sqrt{3}\pi\, a_Q R^2 - 4\pi\, k_V\, R^3 \qquad (6)$$

For a given cross section of the tube structure (Figure 2), the rod radius R includes the thickness of the lipid monolayer and the radius of the water channel. The lipid length, l, was calculated from the equation[43a]

$$f_L = 2\sigma\,(l/a_Q) + \frac{4}{3}\pi\chi\,(l/a_Q)^3 \qquad (7)$$

where the constants for the Q^{224} cubic phase are $\sigma = 1.919$ and $\chi = -2$, and f_L is the lipid volume fraction defined by eq 3. The partial specific volume of MO, v_L, is 1.06 cm^3/g at 20 °C and its temperature dependence is[21d] $v_L(T) = v_L{}^{20}\,[1-9\times10^{-4}\,(T-20)]$. The partial specific volume of water, v_w, is 1.0 cm^3/g.

The temperature dependence of the mean curvature, $\langle C_L\rangle$, determined at the MO headgroup region (eq 4), is presented in Figure 9 (squares). The figure shows that the curvature of the lipid monolayer/water interface in the bicontinuous cubic phase is nearly constant up to about 30 °C and begins to increase above this temperature. Thus, the decrease of a_Q upon heating above 30 °C is certainly associated with an increase in the curvature of the lipid monolayers[42] in the nonlamellar structure.

Acknowledgment. A.A. thanks Dr. Philippe Lainé for interesting discussions and experimental facilities. This work was supported by a grant from the National Science Foundation (project F-618) and by a NATO Grant No. HTECH.LG 971221. The helpful criticism of the reviewers is gratefully acknowledged.

References and Notes

(1) (a) Dhanabalan, A.; Dos Santos, D. S., Jr.; Mendonça, C. R.; Misoguti, L.; Balogh, D. T.; Giacometti, J. A.; Zilio, S. C.; Oliveira, O. N., Jr. *Langmuir* **1999**, *15*, 4560−4564. (b) Sun, K.; Mauzerall, D. *J. Phys. Chem. B* **1998**, *102*, 6440−6447. (c) Matzinger, S.; Hussey, D. M.; Fayer, M. D. *J. Phys. Chem. B* **1998**, *102*, 7216−7224.

(2) (a) Pevenage, D.; Van der Auweraer, M.; De Schryver, F. C. *Langmuir* **1999**, *15*, 8465−8473. (b) Vaes, A.; Van der Auweraer, M.; Bosmans, P.; De Schryver, F. C. *J. Phys. Chem. B* **1998**, *102*, 5451−5459. (c) Prabhananda, B. S.; Kombrabail, M. H. *J. Phys. Chem. B* **1998**, *102*, 8619−8628.

(3) (a) Dhanabalan, A.; Gaffo, L.; Barros, A. M.; Moreira, W. C.; Oliveira, O. N., Jr. *Langmuir* **1999**, *15*, 3944−3949. (b) Mendonça, C. R.; Dhanabalan, A.; Balogh, D. T.; Misoguti, L.; dos Santos, D. S.; Pereira-da-Silva, M. A.; Giacometti, J. A.; Zilio, S. C.; Oliveira, O. N., Jr. *Macromolecules* **1999**, *32*, 1493−1499.

(4) (a) Pevenage, D.; Van der Auweraer, M.; De Schryver, F. C. *Langmuir* **1999**, *15*, 4641−4647. (b) Laguitton-Pasquier, H.; Van der Auweraer, M.; De Schryver F. C. *Langmuir* **1998**, *14*, 5172−5183. (c) Gretchikhine, A.; Schweitzer, G.; Van der Auweraer, M.; De Keyzer, R.; Vandenbroucke, D.; De Schryver, F. C. *J. Appl. Phys.* **1999**, *85*, 1283−1293.

(5) (a) Leblanc, R. M., Salesse, C., Eds.; *Proceedings of the 6th International Conference on Organized Molecular Films*; Trois-Rivieres, Canada, 1993; Elsevier: Amsterdam, 1994 (also in *Thin Solid Films* **1994**, 242−244). (b) Gabrielli, G.; Rustichelli, F. *Proceedings of the 7th International Conference on Organized Molecular Films*; Ancona, Italy, 1995; Elsevier: Amsterdam, 1996 (also in *Thin Solid Films* **1996**, 284−285).

(6) (a) Vuorimaa, E.; Belovolova, L. V.; Lemmetyinen, H. *J. Luminescence* **1997**, *71*, 57−63. (b) Akinin, M.; Tkachenko, N. V.; Lemmetyinen, H. *Langmuir* **1997**, *13*, 3002−3008. (c) Tkachenko, N. V.; Hynninen, P. H.; Lemmetyinen, H. *Chem. Phys. Lett.* **1997**, *261*, 234−240. (d) Ballet, P.; Van der Auweraer, M.; De Schryver, F. C.; Lemmetyinen, H.; Vuorimaa, E. *J. Phys. Chem.* **1996**, *100*, 13 701.

(7) (a) Dhanabalan, A.; Riul, A.; Mattoso, L. H. C.; Oliveira, O. N., Jr. *Langmuir* **1997**, *13*, 4882−4886. (b) Dhanabalan, A.; Riul, A.; Oliveira, O. N., Jr. *Supramol. Sci.* **1998**, *5*, 75−81. (c) Cavalli, A.; Borissevitch, G.; Tabak, M.; Oliveira O. N., Jr. *Thin Solid Films* **1996**, *285*, 731−734. (d) Ionov, R.; Angelova, A. *Sens. Actuators, A* **1995**, *51*, 97−101.

(8) (a) Kruk, J.; Strzalka, K.; Leblanc, R. M. *J. Photochem. Photobiol. B* **1993**, *19*, 33−38. (b) Wang, S.; Leblanc, R. M.; Arias, F.; Echegoyen, L. *Langmuir* **1997**, *13*, 1672−1676. (c) Guay, D.; Leblanc, R. M. *Langmuir* **1987**, *3*, 575−580. (d) Es−Sounni, A.; Leblanc, R. M. *Langmuir* **1992**, *8*, 1578−1581; Ghaicha, L.; Leblanc, R. M.; Villamanga, F.; Chattopadhyay, A. K. *Langmuir* **1995**, *11*, 585−590.

(9) (a) Angelova, A.; Van der Auweraer, M.; Ionov, R.; Vollhardt, D.; De Schryver, F. C. *Langmuir* **1995**, *11*, 3167−3176. (b) Ionov, R.; Angelova, A. *J. Phys. Chem.* **1995**, *99*, 17 593−17 605. (c) Ionov, R.; Angelova, A. *J. Phys. Chem.* **1995**, *99*, 17 606−17 614. (d) Ionov, R.; Angelova, A. *Phys. Rev. E* **1995**, *52*, R21−R24. (e) Angelova, A.; Ionov,

R. *Langmuir* **1996**, *12*, 5643−5653. (f) Angelova, A. *Thin Solid Films* **1994**, *243*, 394−398. (g) Angelova, A.; De Coninck, J.; Ionov, R. *Supramolecular Sci.* **1997**, *4*, 207−214.

(10) (a) Dutta, A. K.; Salesse, C. *Langmuir* **1997**, *13*, 5401−5408. (b) Maloney, K. M.; Grandbois, M.; Salesse, C.; Grainger, D. W.; Reichert, A. *J. Mol. Recognit.* **1996**, *9*, 368−374. (c) Van der Auweraer, M.; Ballet, P.; De Schryver, F. C.; Kowalczyk, A. *Chem. Phys.* **1994**, *187*, *399*. (d) Verschuere, B.; Van der Auwerarer, M.; De Schryver, F. C. *Thin Solid Films* **1994**, *244*, 995−1000. (e) Dutta, A. K. *Langmuir* **1997**, *13*, 5678−5684. (f) Dutta, A. K. *Langmuir* **1998**, *14*, 3036−3040. (g) Dutta, A. K. *Langmuir* **1996**, *12*, 5909−5914.

(11) (a) Song, X.; Perlstein, J.; Whitten, D. G. *J. Am. Chem. Soc.* **1997**, *119*, 9144−9159. (b) Ariga, K.; Lvov, Y.; Kunitake, T. *J. Am. Chem. Soc.* **1997**, *119*, 2224−2231. (c) Shimomura, M. *Prog. Polym. Sci*. **1993**, *18*, 295.

(12) (a) Kimizuka, N.; Wakiyama, T., Miyauchi, H.; Yoshimi, T.; Tokuhiro, M.; Kunitake, T. *J. Am. Chem. Soc.* **1996**, *118*, 5808−5809. (b) Karthaus, O.; Ijiro, K.; Shimomura, M.; Hellmann, Irie, M. *Langmuir* **1996**, *12*, 6714−6716. (c) Moss, R. A.; Jiang, W. *Langmuir* **1997**, *13*, 4498−4501.

(13) (a) Shimomura, M.; Oguchi, M.; Kasuga, K.; Fujii, K.; Shinohara, S.; Kondo, N.; Tajiima, N.; Koshiishi, K. *Thin Solid Films* **1994**, *243*, 358−360. (b) Karthaus, O.; Hioki, M.; Shimomura, M. *Colloids Surf. A* **1997**, *126*, 181−188. (c) Shimomura, M.; Aiba, S.; Tajima, N.; Inoue, N.; Okuyama, K. *Langmuir* **1995**, *11*, 969.

(14) (a) Lvov, Y.; Ariga, K.; Ichinose, I.; Kunitake, T. *J. Am. Chem. Soc.* **1995**, *117*, 6117−6123. (b) Kimizuka, N.; Kawasaki, T.; Hirata, K.; Kunitake, T. *J. Am. Chem. Soc.* **1995**, *117*, 6360−6361. (c) Shishido, A.; Tsutsumi, O.; Kanazawa, A.; Shiono, T.; Ikeda, T.; Tamai, N. *J. Am. Chem. Soc*. **1997**, *119*, 7791−7796.

(15) Clapp, P. J.; Armitage, B.; Roosa, P., O'Brien, D. F. *J. Am. Chem. Soc*. **1994**, 116, 9166−9173.

(16) Shimomura, M.; Karthaus, O.; Ijiro, K. *Synth. Metals* **1996**, 251−257.

(17) Seddon, J. M.; Templer, R. H. Polymorphism of Lipid−Water Systems. In *Structure and Dynamics of Membranes: from Cells to Vesicles*; Lipowsky, R., Sackmann, E. ,Eds.; Elsevier: Amsterdam, 1995, Chapter 3, Vol. 1, pp 97−159.

(18) Lasic, D. D. *Liposomes: From Physics to Applications*; Elsevier: Amsterdam, 1993.

(19) (a) Chiruvolu, S.; Warriner, H.; Naranjo, E.; Idziak, S. H. J.; Rädler, J. O.; Plano, R. J.; Zasadzinski, J. A.; Safinya, C. R. *Science* **1994**, *266*, 1222−1225. (b) Kimizuka N.; Kawasaki, T.; Hirata, K.; Kunitake, T. *J. Am. Chem. Soc*. **1995**, *117*, 6360−6361. (c) Spector, M. S.; Easwaran, K. R. K.; Jyothi, G.; Selinger, J. V.; Singh, A.; Schnur, J. M. *Proc. Natl. Acad. Sci. U.S.A.* **1996**, *93*, 12 943−12 946. (d) Khazanovich, N.; Granja, J. R.; McRee, D. E.; Milligan, R. A.; Reza Ghadiri, M. *J. Am. Chem. Soc*. **1994**, *116*, 6011−6012.

(20) (a) Gruner, S. M. In *Structure of Biological Membranes*; Yeagle, P. L., Ed.; CRC Press: Boca Raton, FL.; 1992; pp 211−250. (b) Tate, M. W.; Eikenberry, E. F.; Turner, D. C.; Shyamsunder, E.; Gruner, S. M., *Chem. Phys. Lipids* **1991**, *57*, 147−164.

(21) (a) Luzzati, V.; Delacroix, H.; Gulik, A.; Gulik-Krzywicki, T.; Mariani, P., Vargas, R. In *Lipid Polymorphism and Membrane Properties*; Epand, R. M., Ed.; Academic Press: San Diego; 1997; pp 3−24. (b) Luzzati, V. *Curr. Opin. Struct. Biol*. **1997**, *7*, 661−668. (c) Mariani, P.; Luzzati, V.; Delacroix, H. *J. Mol. Biol*. **1988**, *204*, 165−189. (d) Luzzati, V. *J. Phys. II France* **1995**, *5*, 1649−1669.

(22) Razumas, V.; Kanapienienė, J.; Nylander, T.; Engström, S.; Larsson, K., *Anal. Chim. Acta* **1994**, *289*, 155−162.

(23) (a) Srisiri, W.; Sisson, T. M.; O'Brien, D. F.; McGrath, K. M.; Han, Y.; Gruner, S. M. *J. Am. Chem. Soc.* **1997**, *119*, 4866−4873. Srisiri, W.; Benedicto, A.; O'Brien, D. F.; Trouard, T. P.; Orädd, G.; Persson, S.; Lindblom, G. *Langmuir* **1998**, *14*, 1921−1926. (c) Blume, A. *Chem. Phys. Lipids* **1991**, *57*, 253−273. (d) Rhodes, D. G.; Blechner, S. L.; Yager, P.; Schoen, P. *Chem. Phys. Lipids* **1988**, *49*, 39−47.

(24) Angelova, A.; Ionov, R. *Langmuir* **1999**, *15*, 7199−7207.

(25) (a) Paternostre, M.; Viard, M.; Meyer, O.; Ghanam, M.; Ollivon, M.; Blumenthal, R. *Biophys. J.* **1997**, *72*, 1683−1694. (b) Ouadahi, S.; Paternostre, M.; Andre, C.; Genin, I.; Thao, T. X.; Puisieux, F.; Devissaguet, J. P.; Barratt, G. *J. Drug Target.* **1998**, *5*, 365−378. (c) Paternostre, M.; Meyer, O.; Grabielle-Madelmont, C.; Lesieur, S.; Ghanam, M.; Ollivon, M. *Biophys. J*. **1995**, *69*, 2476−2488. (d) Pott, T.; Paternostre, M.; Dufourc, E. J. *Eur. Biophys. J*. **1998**, *27*, 237−245.

(26) (a) Grabielle-Madelmont, C.; Hochapfel, A.; Ollivon, M. *J. Phys. Chem. B* **1999**, *103*, 4534−4548. (b) De Oliveira, M. C.; Fattal, E.; Couvreur, P.; Lesieur, P.; Bougaux, C.; Ollivon, M.; Dubernet, C. *Biochim. Biophys. Acta* **1998**, *1372*, 301−310. (c) Forte, L.; Andrieux, K.; Keller, G.; Grabielle-Madelmont, C.; Lesieur, S.; Paternostre, M.; Ollivon, M.; Bourgaux, C.; Lesieur P. *J. Therm. Anal*. **1998**, *51*, 773−782.

(27) (a) Hinzmann, J. S.; McKenna, R. L.; Pierson, T. S.; Han, F.; Kézdy, F. J., Epps, D. E. *Chem. Phys. Lipids* **1992**, *62*, 123−138. (b) Pedersen, S.; Jørgensen, K.; Bækmark, T. R.; Mouritsen, O. G. *Biophys. J*. **1996**, *71*, 554−560. (c) Reyes Mateo, C.; Souto, A. A.; Amat-Guerri F.; Ulises Acuna A. *Biophys. J*. **1996**, *71*, 2177−2191. (d) Epps, D. E.; Wilson, C. L.; Vosters, A. F., Kézdy, F. J. *Chem. Phys. Lipids* **1997**, 121−133. (e) Langner, M.; Hui, S. W. *Chem. Phys. Lipids* **1993**, *65*, 23−30. (f) Bondar, O. P.; Rowe E. S. *Biophys. J*. **1999**, *76*, 956−962.

(28) (a) Epand, R. M.; Leon, B. T.-C. *Biochemistry* **1992**, *31*, 1550−1554. (b) Li, L.; Zheng, L. X.; Yang, F. Y. *Chem. Phys. Lipids* **1995**, *76*, 135−144.

(29) (a) Parasassi, T.; De Stasio, G.; Ravagnan, G.; Rusch, R. M.; Gratton, E. *Biophys. J*. **1991**, *60*, 179−189. (b) Sassaroli, M.; Vaukhonen, M.; Somerharju, P.; Scarlata, S. *Biophys. J*. **1993**, *64*, 137−149. (c) Bramhall, J. *Biochemistry* **1986**, *25*, 3479−3486.

(30) (a) Epand, R. F., Kraayenhof, R.; Sterk, G. J.; Wong Fong Sang, H. W.; Epand, R. M. *Biochim. Biophys. Acta* **1996**, *1284*, 191−195. (b) Hong, K.; Baldwin, P. A.; Allen, T. M.; Papahadjopoulos, D. *Biochemistry* **1988**, *27*, 3947−3955. (c) Epand, R. M. *J. Fluorescence* **1995**, *5*, 3−8; Cheng, K. H. *Chem. Phys. Lipids* **1990**, *53*, 191−202. Han, X.; Gross, R. W. *Biophys. J*. **1992**, *63*, 309−316.

(31) Phenylethynyl-fluorophore compounds[32] are of increasing research interest because of their functions as good chemiluminescence activators, fluorescent labels of polymer latexes, dyes for development of organic third-order nonlinear optical materials, selective antagonists at human A(3) adenosine receptors, materials for use in electron-transfer processes, electrophotographic fluorescent toner preparations, etc.[32,33]

(32) (a) Nakatsuji, S.; Matsuda, K.; Uesugi, Y.; Nakashima, K.; Akiyama, S.; Fabian, W. *J. Chem. Soc. Perkin Trans. 1* **1992**, (7), 755−758. (b) Lukacs, J.; Lampert, R. A.; Metcalfe, J.; Phillips, D. *J. Photochem. Photobiol. A: Chem*. **1992**, *63*, 59−65. (c) Nakamura, H.; Chun, W.; Takeuchi, D.; Murai, A. *Tetrahedron Lett*. **1998**, *39*, 301−304. (d) Nguyen, P.; Todd, S.; Van den Biggellaar, D.; Taylor, N.; Marder, T. B.; Wittmann, F.; Friend, R. H. *Synlett* **1994**, (4), 299−301.

(33) (a) Taniike, K.; Katayama, N.; Sato, T.; Ozaki, Y.; Czarnecki, M. A.; Satoh, M.; Watanabe, T.; Yasuda, A. *Mikrochimika Acta*, **1997**, Suppl. 14, 581−583. (b) Jiang, J. L.; Vanrhee, A. M.; Chang, L.; Patchornik, A., Ji, X. D.; Evans, P.; Melman, N.; Jacobson, K. A. *J. Medicinal Chem*. **1997**, *40*, 2596−2608.

(34) (a) Angelova, A.; Petrov, J. G.; Kuleff, I. *Langmuir* **1992**, *8*, 213−216. (b) Angelova, A.; Petrov, J. G.; Dudev, T.; Galabov, B. *Colloids and Surfaces* **1991**, *60*, 351−368. (c) Angelova, A.; Peñacorada, F.; Stiller, B.; Zetzsche, T.; Ionov, R.; Kamusewitz, H.; Brehmer, L. *J. Phys. Chem*. **1994**, *98*, 6790−6796. (d) Petrov, J. G.; Angelova, A. *Langmuir* **1992**, *8*, 3109−3115.

(35) Almgren, M.; Grieser, F.; Thomas, J. K. *J. Am. Chem. Soc*. **1979**, *101*, 279−291.

(36) (a) *CRC Handbook of Chemistry and Physics*, 74th ed.; Lide, D. R., Ed.; CRC Press: Boca Raton, 1994; p 8/57. (b) *Solvent Guide*. Burdick and Jackson Laboratories, Inc., Muskegon: Michigan, 1980; p 129.

(37) (a) Kimura, Y.; Ikegami, A. *J. Membrane Biol*. **1985**, *85*, 225−231. (b) Ohki, S.; Arnold, K. *J. Membrane Biol*. **1990**, *114*, 195−203. (c) Fernandez, M. S.; Fromherz, P. *J. Phys. Chem*. **1977**, *81*, 1755−1761. (d) McIntosh, T. J. *Chem. Phys. Lipids* **1996**, *81*, 117−131. (e) Rand, R. P.; Parsegian, V. A. *Biochim. Biophys. Acta* **1989**, *988*, 351−376.

(38) (a) Tate, M. W.; Gruner, S. M. *Biochemistry* **1989**, *28*, 4245−4253. (b) Turner, D. C.; Gruner, S. M. *Biochemistry* **1992**, *31*, 1340−1355. (c) Angelov, B.; Ollivon, M.; Angelova, A. *Langmuir* **1999**, *15*, 8225−8234.

(39) (a) Erbes, J.; Czeslik, C.; Hahn, W.; Winter, R.; Rappolt, M.; Rapp, G. *Ber. Bunsen-Ges. Phys. Chem*. **1994**, *98*, 1287−1293. (b) Angelova, A.; Ionov, R.; Koch M. H. J.; Rapp, G. *Archives Biochem. Biophys* **2000**, *378*, 93−106.

(40) (a) Czeslik, C.; Winter, R.; Rapp, G.; Bartels, K. *Biophys. J*. **1995**, *68*, 1423−1429. (b) Hyde, S. T.; Andersson, S.; Ericsson, B.; Larsson, K. *Zeitschrift f. Kristallographie* **1984**, 168, 213-219. (c) Caffrey, M. *Biochemistry*, **1987**, *26*, 6349−6363. (d) Chung, H.; Caffrey, M. *Nature* **1994**, *368*, 224−226.

(41) (a) Tardieu, A.; Luzzati, V.; Reman, F. C. *J. Mol. Biol*. **1973**, *75*, 711−733. (b) Rapp, G.; Rappolt, M.; Laggner, P. *Prog. Colloid Polym. Sci*. **1993**, *93*, 25−29. (c) Janiak, M. J.; Small, D. M.; Graham Shipley, G. *Biochemistry* **1976**, *15*, 4575−4580. (d) Katsaras, J.; Raghunathan, V. A.; Duforc, E. J.; Duforcq, J. *Biochemistry* **1995**, *34*, 4684−4688.

(42) (a) Gruner, S. M. *J. Phys. Chem*. **1989**, *93*, 7562−7570. (b) Gruner, S. M. *Proc. Natl Acad. Sci. USA*. **1985**, *82*, 3665−3669. (c) Marsh, D. *Biophys. J*. **1996**, *70*, 2248−2255. (d) Kirk, G. L.; Gruner, S. M.; Stein, D. L. *Biochemistry* **1984**, *23*, 1093−1102. (e) Gruner, S. M.; Tate, M. W.; Kirk, G. L.; So, P. T. C.; Turner, D. C.; Keane, D. T.; Tilcock, C. P. S.; Cullis, P. R. *Biochemistry* **1988**, *27*, 2853−2866.

(43) (a) Turner, D. C.; Wang, Z.-G.; Gruner, S. M.; Mannock, D. A.; McElhaney, R. N. *J. Phys. II France* **1992**, *2*, 2039−2063. (b) Luzzati, V. In *Biological Membranes*; Chapman, D., Ed.; Academic Press: London, Vol. 1, 1968; pp 71−123. (c) Gulik, A.; Luzzati, V.; De Rosa, M.; Gambacorta, A. *J. Mol. Biol*. **1985**, *182*, 131−149.